Chemical Engineering   Engineering

Fall 12-9-2019

Pd-Fe3O4/RGO: a Highly Active and Magnetically Recyclable Catalyst for Suzuki Cross Coupling Reaction using a Microfluidic Flow Reactor

Hany A. Elazab
The British University in Egypt, hany.elazab@bue.edu.eg

Research Article

Pd-Fe₃O₄/RGO: a Highly Active and Magnetically Recyclable Catalyst for Suzuki Cross Coupling Reaction using a Microfluidic Flow Reactor

Hany A. Elazab[1*], Ali R. Siamaki[2], B. Frank Gupton[2,3], M. Samy El-Shall[2,3]

[1]Chemical Engineering Department, The British University in Egypt, BUE, Cairo, Egypt
[2]Chemical Engineering Department, Virginia Commonwealth University, Richmond, VA, United States of America.
[3]Chemistry Department, Virginia Commonwealth University, Richmond, VA, United States of America

Abstract

There are several crucial issues that need to be addressed in the field of applied catalysis. These issues are not only related to harmful environmental impact but also include process safety concerns, mass and heat transfer limitations, selectivity, high pressure, optimizing reaction conditions, scale-up issues, reproducibility, process reliability, and catalyst deactivation and recovery. Many of these issues could be solved by adopting the concept of micro-reaction technology and flow chemistry in the applied catalysis field. A microwave assisted reduction technique has been used to prepare well dispersed, highly active Pd/Fe₃O₄ nanoparticles supported on reduced graphene oxide nanosheets (Pd-Fe₃O₄/RGO), which act as a unique catalyst for Suzuki cross coupling reactions due to the uniform dispersion of palladium nanoparticles throughout the surface of the magnetite - RGO support. The Pd-Fe₃O₄/RGO nanoparticles have been shown to exhibit extremely high catalytic activity for Suzuki cross coupling reactions under both batch and continuous reaction conditions. This paper reported a reliable method for Suzuki cross-coupling reaction of 4-bromobenzaldehyde using magnetically recyclable Pd/Fe₃O₄ nanoparticles supported on RGO nanosheets in a microfluidic-based high throughput flow reactor. Organic synthesis can be performed under high pressure and temperature by using a stainless steel micro tubular flow reactor under continuous flow reaction conditions. Optimizing the reaction conditions was performed via changing several parameters including temperature, pressure, and flow rate. Generally, a scalable flow technique by optimizing the reaction parameters under high-temperature and continuous reaction conditions could be successfully developed. Copyright © 2019 BCREC Group. All rights reserved

How to Cite: Elazab, H.A., Siamaki, A.R., Gupton, B.F., El-Shall, M.S. (2019). Pd-Fe₃O₄/RGO: a Highly Active and Magnetically Recyclable Catalyst for Suzuki Cross Coupling Reaction using a Microfluidic Flow Reactor. *Bulletin of Chemical Reaction Engineering & Catalysis*, 14(3): 478-489 (doi:10.9767/bcrec.14.3.3518.478-489)

1. Introduction

Over the past few decades, micro-reaction technology has been emerged as an ideal route to solve several critical issues in many aspects including organic chemistry and applied catalysis [1-8]. This new technology has created new promising horizons for chemical synthesis and industry via performing chemistry under continuous flow reaction conditions instead of the conventional batch chemistry [9-16]. This

---

* Corresponding Author.
  E-mail: elazabha@vcu.edu (H.A. Elazab);

newly adopted approach could achieve a significant improvement via using safer micro-reactor processes [17-26]. This will definitely improve the capability of producing smaller scale synthetic chemicals on demand and on site at which those products are urgently needed as well [27-29]. There are many challenges in the field of chemical industry like pollution, environmental issues, process safety, and scale-up issues that could be minimized via using micro-reactor technology [30-32]. Palladium-catalyzed coupling reactions are among the most widely applied reactions in the field of organic synthesis although there are some disadvantages of using palladium in such reactions including its high price and also the high toxicity of the metal residue which is considered as a critical issue, especially in the field of pharmaceutical industry [30-35]. Those disadvantages could be minimized by using very small amounts of palladium catalysts, however, there will be still some issues associated with homogeneous catalysis like the lack of recyclability and contamination from residual metals in the reaction products [20-22,24-28]. The key for solving this technical problem could be simply by using heterogenized homogeneous catalyst or heterogeneous catalyst as it is widely known. Heterogeneous catalysis has economic and environmental advantages if compared to the stoichiometric reactions due to the catalyst increasing ability of being easily separated and recycled [26-46].

Nanotechnology is widely used in several catalysis applications as the particles at the nano scale can dramatically increase the exposed surface area of the active component of the catalyst, hence enhancing the contact between reactants and catalyst in a way similar to that of the homogeneous catalysts. The use of magnetic nanoparticles in such catalytic system has tremendous advantages including high catalytic activity, ease of recovery using an external magnetic field and the possibility of using water as a solvent as well. Those proposed catalytic systems can be simply transition metal catalysts such as palladium, copper, ruthenium, and nickel, which are used on silica, magnetic nanoparticles, polymers, and carbon based supports. Cross coupling, reactions are among the most strategic processes in the field of organic synthesis as they have many applications in pharmacy, agriculture, medicine, cosmetics and natural products.

Carbon based materials like graphene are generally considered as an ideal candidate for being used as supports for several catalysts as a result of their huge surface area, limited interaction with the metal catalysts, besides other attractive features including thermal, chemical stability, and easy recovery of noble metals like palladium from the spent catalysts. Also, the structural defects in graphene create new surface functionalities that enhance the interactions with the anchored metal nanoparticles. Recently, although the synthesis and applications of magnetic nanoparticles (MNPs) of noble metal nanoparticles supported on graphene is still considered as a new area of research but it has attracted more interest in catalysis research and have been used in some industrially important reactions.

Although carbon materials has an increasing importance to be used as catalyst supports but there is also an endless research efforts to develop other alternative kinds of supports including metal oxides. It is expected that this work provides a significant step toward the development of new clean technologies for organic synthesis. This work is a kind of enhancement of our previously work in preparing palladium- magnetite nanoparticles supported on graphene (Pd-Fe$_3$O$_4$/RGO) under batch reaction conditions.

The main purpose of this scientific research is to investigate the catalytic performance of the prepared catalyst under flow reaction conditions through immobilization of the palladium based catalyst into a cartridge, to be used on a microfluidic flow reactor. The use of a microfluidics-based flow reactor (X-Cube™) offers a potential solution for the previously mentioned issues. It also provides a safe and easy use of immobilized catalysts placed in CatCart™ cartridges. Moreover, this technique enables the synthesis of several chemical products in a short time through optimization of the reaction conditions in just few minutes. Herein, It was reported the results on the cross-coupling reactions of bromobenzaldehyde in the presence of phenyl boronic acid carried out in the flow reactor X-Cube™ using Pd-Fe$_3$O$_4$/RGO catalyst. A detailed investigation of the effects of the changes in the reaction conditions (temperature, flow rate) has been carried out.

2. Materials and Methods

2.1 Chemicals and Reagents

All chemicals used in our experimental procedure were used as received without any further purification. Palladium nitrate (10 wt. % in 10 wt. % HNO$_3$, 99.999%) and hydrazine hydrate (80%, Hydrazine 51%) were purchased

from Sigma Aldrich. Deionized water (D.I. H_2O) was used for all experiments, while high-purity graphite powder (99.9999%, 200 mesh) was purchased from Alfa Aesar. Aryl bromide, bromobenzene and potassium carbonate were also purchased from Aldrich and used as received.

2.2 Catalyst Characterization and Product Compositions

TEM images were captured using JEOL electron microscope. X-ray photoelectron spectroscopy (XPS) analysis was implemented on a Thermo Fisher Scientific ESCALAB, while X-ray diffraction patterns were identified using X'Pert PRO PANanalytical X-ray diffraction unit at room temperature. GC–MS measurements were performed on Agilent gas chromatograph equipped with a mass selective detector.

A continuous flow reactor named ThalesNano X-Cube™ is used in order to perform chemical reactions under inert conditions, temperatures up to 200 °C and pressures up to 150 bar. It has been recently reported that carbon-carbon reactions formation is more efficient using X-Cube™ in comparison to batch mode. The reaction solvent was allowed to flow through the X-Cube™ system for 10 minutes in order to equilibrate the filled CatCart cartridge, where

the catalyst was previously loaded using a manual piston. A sample of the starting materials in the reaction solvent was pumped through the X-Cube™, the total amount of product mixture was collected to sample vial and the column was washed with the eluent to remove any material still absorbed to the Cat-Cart; the product mixture was analyzed by GC-MS.

2.3 Graphene Oxide Synthesis

The modified Hummers and Offeman method was used to prepare graphene oxide. In typical synthesis, high purity graphite powder (99.9999%, 200 mesh) was oxidized using a mixture of $H_2SO_4/KMnO_4$. Graphite (4.5 g, 0.375 mol) and $NaNO_3$ (2.5 g, 0.0294 mol) were mixed in a conical flask, while the mixture was then maintained in an ice bath.

Concentrated H_2SO_4 (115 mL, 2.157 mol) was added under continuous stirring while $KMnO_4$ (15 g, 0.095 mol) was then slowly added over a time period of 2.5 h. Deionized water (230 mL) was slowly added to the previous mixture and once the mixture temperature became stable it was kept around 80 ºC. Then, after 20 min., deionized water (700 mL) was added followed by drop wise addition of (10%) H_2O_2 (20 mL, 0.667 mol). The resulting yellowish-
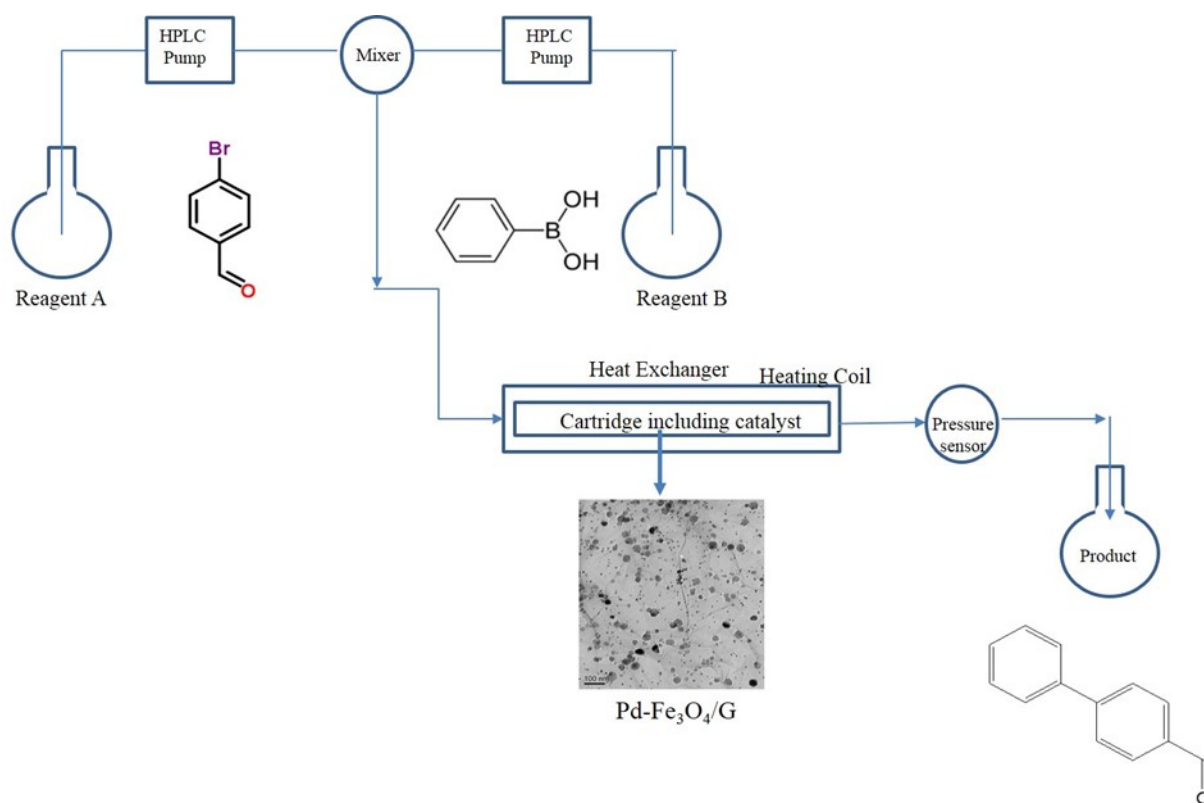
**Scheme 1.** High-temperature/pressure capillary flow reactor

brown cake of solid was washed using 1M HCl and then washed with hot deionized water. The graphite oxide powder was then dried under vacuum overnight. Resultant graphite oxide could be readily exfoliated to completely water dispersed graphene oxide (GO) by ultra-sonication.

2.4 Synthesis of Graphene Supported Pd-Fe₃O₄ Catalyst to be Loaded into Catridge™

Graphene oxide (GO) was used as an ideal support for the catalyst preparation. In typical synthesis, GO (60 mg) was dispersed in 50 mL of water for 1 h to produce an aqueous dispersion of graphene oxide using a sonication bath. Then, deionized water (50 mL) in which appropriate amount of Palladium nitrate (10 wt. % in 10 wt. % HNO_3, 99.999%, 200 μL) and Fe $(NO_3)_3.9H_2O$ (190.5 mg, 0.471 mmol) were added and sonicated for another 1 h. The solution was added to the aqueous dispersion of graphene oxide (GO) while maintaining stirring. After stirring the whole mixture for 3 h, the reducing agent hydrazine hydrate (2 mL) was added at room temperature and the solution was immediately heated via using a microwave for (120) s and the color was then changed to dark black color, indicating the complete chemical reduction. Hence, the final product was washed with hot deionized water 3-5 times; ethanol 2-3 times, and then dried in oven at 80 °C.

2.5 General Procedure for Suzuki Cross-Coupling under Flow Reaction Conditions

Aryl bromide (0.51 mmol, 1 eq.) was dissolved in a mixture of 4 mL H_2O: EtOH (1:1)
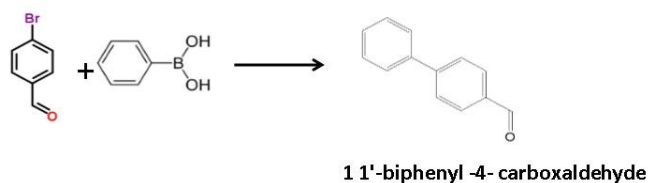
Scheme 2. Suzuki cross-coupling reaction with Pd-Fe₃O₄/RGO

and placed in a 10-mL microwave tube. Then, aryl boronic acid (0.61 mmol, 1.2 eq.) and Potassium carbonate (1.53 mmol, 3 eq.) were added, and finally the resulting mixture is introduced to flow continuously over the palladium-magnetite supported on graphene nanoparticles catalyst (Pd-Fe3O4/G) with different tested catalyst loading. The following catalyst amounts (10, 25, 35, 50, and 100 mg) were previously loaded into CatCart cartridge™, and then heating took place at the assigned temperature and time. The progress of the reaction was monitored using GC-MS analysis to an aliquot of the reaction mixture.

3. Results and Discussion

The mechanism of deactivation of the catalyst is mainly due to the formation of aggregated Pd nanoparticles which leads to the decrease in the surface area and saturation of the coordination sites. The palladium content in catalyst was determined by means of inductively coupled plasma (ICP-OES). Palladium content was found to be 9.2 wt % compared to 10 using ICP-OES. After completion of the experiments, the Pd-Fe₃O₄/G was separated from the cartridge for characterization. The reaction solution was analyzed by ICP-MS, and the palladium content in the solution was determined to be 700 ppb. Such a small amount of leached palladium may argue against complete heterogeneity of the catalytic system in this reaction. However, further evidence on the nature of the catalytic mechanism is the failure to observe reactivity after the removal of the supported nanoparticles from the reaction medium.

In Scheme 2, a 4-bromobenzaldehyde was selected instead of bromobenzene that was selected before in our previously published work[64] for two reasons, the first reason is to avoid homo coupling reaction that may occur under these reaction conditions and the second reason is to avoid formation of any solid products that may be produced from this reaction under the reaction conditions which may lead to clogging of tubes of instruments in which the reactants flow over the catalyst. In addition to

Table 1. Conversion percentage using different ratios of solvent systems for Pd-Fe₃O₄/RGO catalyst*

Run	Temperature (ºC)	MW. Time (min.)	Solvent (mL)	Conversion (%)
1	80	10	4	100
2	80	10	4	100
3	80	10	4	100

* Run 1: 0.5 mol. % (Pd-Fe₃O₄/ G) Catalyst – Solvent ($C_2H_5OH : H_2O$ = 1: 1)
* Run 2: 0.5 mol. % (Pd-Fe₃O₄/ G) Catalyst – ($C_2H_5OH : H_2O$: THF = 1 : 1 : 1)
* Run 3: 0.5 mol. % (Pd-Fe₃O₄/ G) Catalyst – ($C_2H_5OH : H_2O$: THF = 1.8 : 1.8 : 0.4) i.e ($C_2H_5OH : H_2O$: THF = 4.5 : 4.5 : 1)

those precautions that were taken into consideration; different ratios of solvent systems were investigated to find the optimum conditions under which we could run the experiment with highest possible conversion. So, as in Table 1, it was possible to obtain 100% conversion by changing the ratios of water, ethanol, and THF to obtain the highest possible conversion with using the minimum amount of THF to make sure that all products will be in liquid form to avoid any undesired solid products that may cause clogging. The change of solvent system was to optimize conditions in order to avoid any blocking in the microreactor channels.

It is obvious from Table 2 below, that the screening experiments that were performed in Table 1 were critical experiments as conversion is changing dramatically according to several factors like reaction temperature, catalyst loading, and the most important factor, which is the

solvent system ratios. Different solvent systems were investigated in order to select the best solvent system that prevent any kind of clogging in the flow reactor as shown in Tables 1 and 2. According to the data collected from previously mentioned experiments in Table 2 along with changing the solvent system ratios and the catalyst loading amount should be varied, it was possible to optimize the reaction conditions as shown in Table 3. Generally, it was found that increasing catalyst loading from 50 mg to 100 mg, increasing temperature and decreasing the flow rate of reaction mixture over the catalyst in the CatCart cartridge enabled us from increasing the conversion percentage. It could be possible to collect about 30 mL of the product with conversion about 100%.

In Table 4, it was found that increasing the reaction temperature from 80 ºC to 100 ºC and decreasing the flow rate from 0.8 mL/min. to

Table 2. Conversion percentage using different reaction temperatures for Pd-Fe$_3$O$_4$/RGO catalyst[*]

Run	Temperature (ºC)	Flow Rate (mL/min.)	Amount (mL)	Conversion (%)
1	80	1	10	53
2	80	1	10	17
3	80	1	10	14
4	80	1	10	13
5	100	0.7	10	31
6	100	0.7	10	15
7	100	0.7	10	14
8	100	0.7	10	13
9	100	0.7	10	9
10	120	0.6	10	18
11	120	0.6	10	15
12	120	0.6	10	12

[*] 50 mg of (Pd-Fe$_3$O$_4$/ G) Catalyst – (C$_2$H$_5$OH : H$_2$O : THF = 1 : 1 : 1)

Table 3. Conversion percentage using 80 ºC reaction temperatures for Pd-Fe$_3$O$_4$/RGO catalyst[*]

Run	Temperature (ºC)	Flow Rate (mL/min.)	Amount (mL)	Residence Time (min.)	Conversion (%)
1	80	0.8	10	12.5	100
2	80	0.8	10	12.5	95
3	80	0.8	10	12.5	87
4	80	0.8	10	12.5	76
5	80	0.8	10	12.5	64
6	80	0.8	10	12.5	59

[*] 100 mg of (Pd-Fe$_3$O$_4$/ G) Catalyst – (C$_2$H$_5$OH : H$_2$O : THF = 4.5 : 4.5 : 1)

0.7 mL/min. did not make any enhancement in conversion percentage, as it was still possible to collect about 28 mL of the product with conversion about 100%.

In Table 5, it was found that maintaining the reaction temperature at 100 ºC and decreasing the flow rate from 0.7 mL/min to 0.6 mL/min make a great enhancement in conversion percentage as it became possible to collect about 60 mL of the product with conversion about 100%.

In Table 6, it was found that maintaining the reaction temperature at 100 ºC and decreasing the flow rate from 0.6 mL/min to 0.5 mL/min decreased the enhancement that was achieved in conversion percentage as it became possible to collect just 40 mL of the product with conversion about 100%. After the reaction has been completed, the catalyst was removed from the cartridge and washed with ethanol and then it is easily removed from catalyst-ethanol mixture via applying an external mag-

Table 4. Conversion percentage using 100 ºC reaction temperatures for Pd-Fe$_3$O$_4$/RGO catalyst*

Run	Temperature (ºC)	Flow Rate (mL/min.)	Amount (mL)	Residence Time (min.)	Conversion (%)
1	100	0.7	10	14	90
2	100	0.7	10	14	86
3	100	0.7	10	14	75
4	100	0.7	10	14	63
5	100	0.7	10	14	55
6	100	0.7	10	14	48
7	100	0.7	10	14	26

* 100 mg of (Pd-Fe$_3$O$_4$/ G) Catalyst – (C$_2$H$_5$OH : H$_2$O : THF = 4.5 : 4.5 : 1)

Table 5. Conversion percentage using 100 ºC reaction temperatures for Pd-Fe$_3$O$_4$/RGO catalyst*

Run	Temperature (ºC)	Flow Rate (mL/min.)	Amount (mL)	Residence Time (min.)	Conversion (%)
1	100	0.6	20	33.3	98
2	100	0.6	20	33.3	97
3	100	0.6	20	33.3	90
4	100	0.6	40	66.6	76
5	100	0.6	20	33.3	62
6	100	0.6	20	33.3	44
7	100	0.6	20	33.3	24

* 100 mg of (Pd-Fe$_3$O$_4$/ G) Catalyst – (C$_2$H$_5$OH : H$_2$O : THF = 4.5 : 4.5 : 1)

Table 6. Conversion percentage using 100 ºC reaction temperatures for Pd-Fe$_3$O$_4$/RGO catalyst†

Run	Temperature (ºC)	Flow Rate (mL/min.)	Amount (mL)	Residence Time (min.)	Conversion* (%)	Conversion** (%)	Conversion*** (%)
1	100	0.5	20	40	100	100	78
2	100	0.5	20	40	96	94	65
3	100	0.5	20	40	46	40	35
4	100	0.5	20	40	20	18	15
5	100	0.5	20	40	20	16	12
6	100	0.5	20	40	20	14	10
7	100	0.5	20	40	17	10	8

† 100 mg of (Pd-Fe$_3$O$_4$/ G) Catalyst – (C$_2$H$_5$OH : H$_2$O : THF = 4.5 : 4.5 : 1)
* Conversion for the catalyst first run.
** Conversion for the catalyst second run.
** Conversion for the catalyst third run

netic field using a strong magnet and washed again several times with ethanol and dried until constant weight in order to be used in the next run.

Table 6 shows that the catalyst performance is decreasing in second and third run compared to the first run due to catalyst deactivation that was confirmed by catalyst TEM image as in Figure 2. Hence, the remaining resulting mixture was finally extracted with CH_2Cl_2 (3 × 50 mL). The organic layers were combined, dried over anhydrous $MgSO_4$, and filtered. The solvent in the filtrate was removed under vacuum to give a solid product which was further puri-

fied by flash chromatography using hexane: ethyl acetate as the eluent. So, from the previous study it was finally deduced that the optimum conditions to evaluate the catalytic activity of Pd-Fe_3O_4 supported on Graphene under continuous flow reaction conditions using Thales Nano X-Cube flow reactor is using 100 mg of catalyst in CatCart cartridge with a flow rate 0.6 mL/min for the reactants over the catalyst under 100 °C as a reaction temperature.

Characterization of the graphene supported Pd-Fe_3O_4 samples prepared by the HH-MWI, method was implemented using several techniques including XRD, XPS, and TEM analyses. Figure 1 displays the XRD patterns of Pd-Fe_3O_4/RGO sample prepared by the simultaneous reduction of GO and palladium nitrate – iron nitrate mixture using HH under MWI.

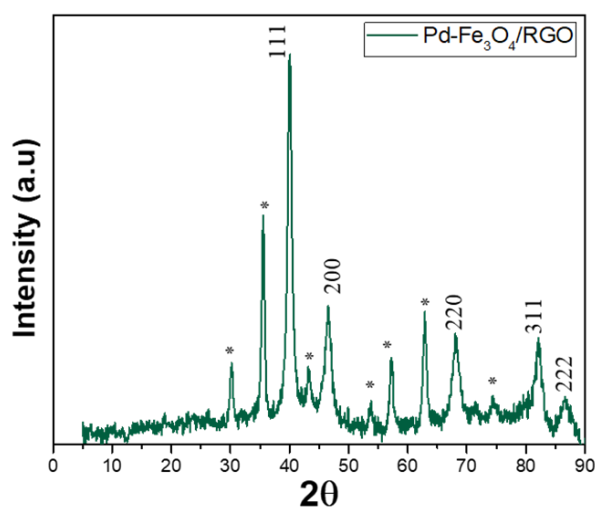**Figure 1.** XRD Pattern of Palladium-Fe_3O_4/RGO catalyst.

Figure 3. Catalyst separation using a strong magnet.

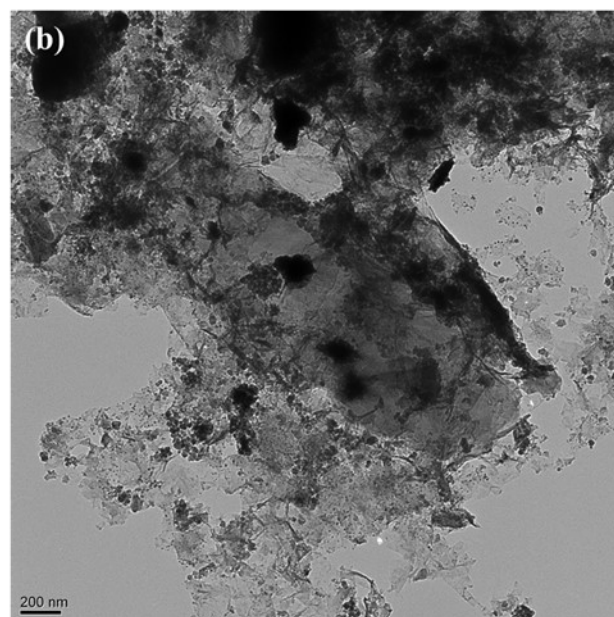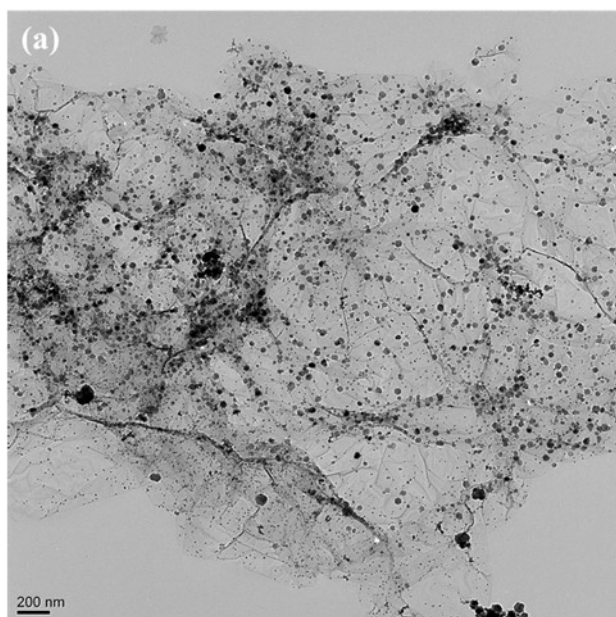**Figure 2.** TEM images of Pd-Fe_3O_4/RGO catalyst; (a) before the reaction, (b) after the reaction when removed from cartridge^{TM}.

There is a very small broad peak around 2θ of 26.7º in the Pd-Fe$_3$O$_4$/G sample that could suggest the presence of a minor component of multilayer graphene. While, the presence of Pd nanoparticles could enhance the interaction among a few graphene layers, the noticed weak intensity of the 2θ of 26.7º peak indicates that the extent of multilayer graphene in the Pd-Fe$_3$O$_4$/RGO sample is insignificant.

Generally, the XRD pattern clearly indicates that the produced catalyst is enriched with Fe$_3$O$_4$ and metal Pd (0). The palladium shows the typical characteristic sharp diffraction peak at 2θ of 40º. The XRD patterns indicate the presence of (Fe$_3$O$_4$) magnetite with reference code (ICDD-00-003-0863). It is remarkable that the sharp diffraction peak at 2θ of 40º which is characteristic to palladium and also the characteristic peak (*) of Fe$_3$O$_4$ is shown as a sharp diffraction peak at 2θ of 35º. The very small

broad peak around 2θ of 26º in Pd-Fe$_3$O$_4$/RGO sample could suggest the presence of a minor component of multilayer graphene.

The diffraction peaks (2θ) of Pd-Fe$_3$O$_4$/RGO at 40, 46.8, and 68.2 are ascribed to the (111), (200), and (220) planed of Pd nanoparticle (NPs) which are similar to pure palladium and also to the peaks of Pd/Fe$_3$O$_4$ as shown.

Figure 2 displays representative TEM images of the Pd-Fe$_3$O$_4$/RGO catalyst before and after reaction. The TEM images show the presence of uniform well-dispersed Pd-Fe$_3$O$_4$ nanoparticles on Graphene. From these TEM images; it is obvious that the catalyst has excellent dispersion of Pd-Fe$_3$O$_4$ on the graphene surface and also it has smaller particle size which is a very important and decisive factor in catalysis. This is very consistent with the catalytic activity data obtained from experimental testing of this catalyst under batch reaction conditions. It is very interesting to note the role of Pd^{+2} in assisting the formation of magnetite nanoparticles onto the surface of the nanosheets of graphene.

Generally, it is clear that palladium presence is a decisive factor in avoiding the agglomeration of products after microwave-assisted reduction of graphene oxide with Fe^{+2} alone using hydrazine hydrate. From these TEM images; it was found that the particle size of Pd was Pd was (4-6 nm) and Fe$_3$O$_4$ was (16-18 nm) as shown in the previously mentioned figure.

Figure 4 shows the unique magnetic properties of the Pd-Fe$_3$O$_4$ supported on Graphene catalyst when using an external magnetic field. The magnetic properties of catalyst were measured using Vibrating Sample Magnetometer (VSM) analysis. Figure 4 presents the magnetic hysteresis loop of Pd/Fe$_3$O$_4$ supported on
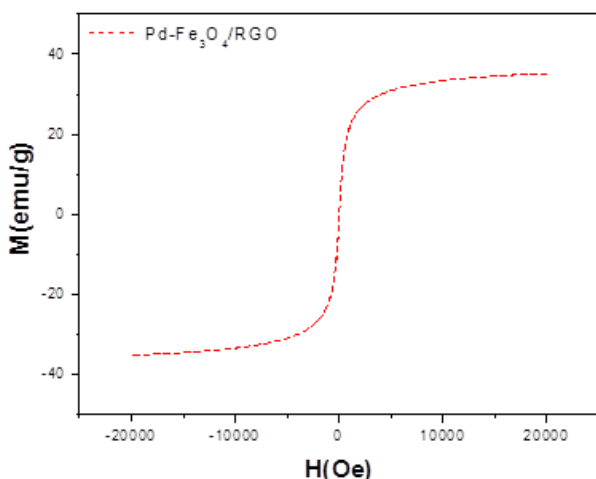

Figure 4. Magnetic hysteresis loops of Pd-Fe$_3$O$_4$ /RGO.
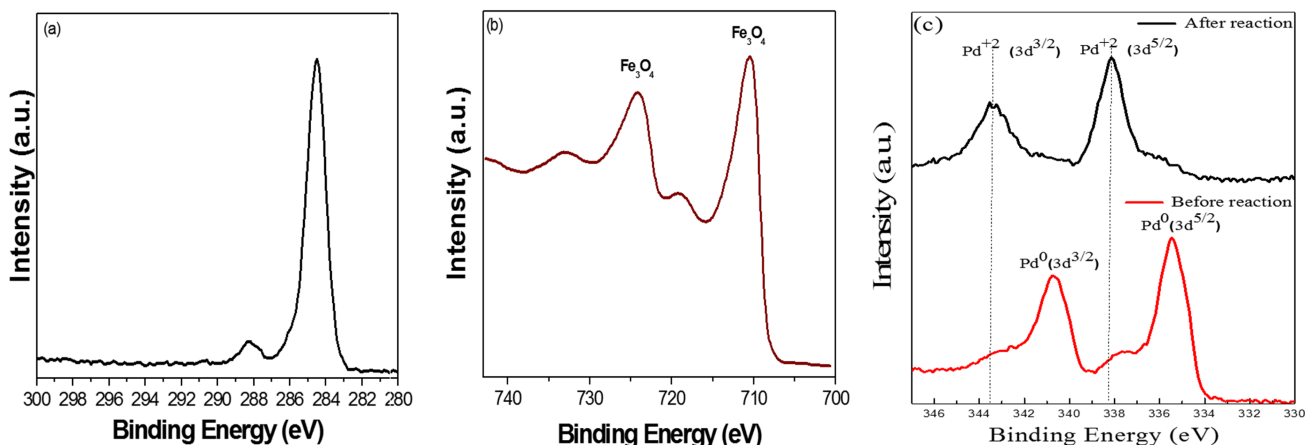

Figure 5. (a) XPS - C 1S, (b) XPS - Fe 2p, (c) XPS - Pd 3d before reaction, (d) XPS - Pd 3d after reaction for Pd/Fe$_3$O$_4$ supported on Graphene.

Graphene. This figure simply shows the hysteresis curves obtained for the prepared catalyst with an applied field sweeping from -20 to 20 kOe.

The obtained hysteresis loop confirmed the super-paramagnetic behavior at room temperature with nearly zero coercivity and extremely low remnant magnetization values. The lack of remaining magnetization while removing the external magnetic field is consistent with the super-paramagnetic behavior observed in the nano-sheets of graphene that were decorated with Pd/Fe_3O_4 nanoparticles.

The XPS technique is more sensitive and reliable technique used for the analysis of the surface oxides compared to XRD. The Pd-Fe_3O_4/G was found to have a C1s binding energy around 284.5 eV as illustrated in Figure 5a. Samples showed that the binding energy (the energy difference between the initial and final states of the photoemission process) of Fe 2P 3/2 was 710.5 eV, indicating that Fe was present as Fe_3O_4 and also the binding energy of Fe 2P 1/2 was 723.7 eV indicating that Fe was present in the oxidation state of Fe_3O_4 as illustrated in Figure 5b. Figure 5c shows that most of Pd is in the form of Pd^0 which besides excellent

dispersion of palladium on graphene surface as shown previously in TEM images is consistent with experimental data that reveals the excellent catalytic activity of the prepared catalyst. The binding energies of Pd $3d^{5/2}$ were 334.8, 335.14 eV, while were 340.1, 340.57 eV for Pd $3d^{3/2}$ corresponding to Pd^0. Similarly; the binding energies of Pd $3d^{3/2}$ was 341.38, 343.2 eV, and Pd $3d^{5/2}$ was 336.23, 337.85 eV corresponding to Pd (II) which as indication that Pd^0 was converted to Pd (II) after reaction was done as shown in Figure 5d.

Actually this is also consistent with the results that confirmed that the catalyst was catalytically deactivated as most of Pd^0 was converted to Pd^{+2}. This deactivation was also due to the agglomeration that was noticed on graphene surface after reaction was done as previously shown in TEM images as in Figures 2a,b. Those TEM images clearly demonstrate the agglomeration and accumulation of the Pd-Fe_3O_4 nanoparticles on the surface of graphene.

Figure 6 gives an overview about the catalyst half life under the optimum reaction conditions that were previously investigated. In this figure, it is obvious that the catalytic activity of the catalyst was very high (about 100% conversion) during the first 90 minutes from starting the reaction and then started to decrease gradually. Table 7 summarizes some of the critical data that was collected in the experimental work done. It gives an overview of the relation between the catalyst loading in (mg) of catalyst and its effect on the conversion percentage under different selected flow rates. Figure 7 gives an overview about the catalyst loading dependency under different reaction conditions. From this figure, it is obvious that decreasing the flow rate for the same catalyst loading lead to an increase in the conversion percentage while

Table 7. Catalyst loading dependency for Pd-Fe_3O_4/RGO catalyst

Catalyst Loading (mg)	Conversion (%)		
	Flow Rate 0.5 mL/min.	Flow Rate 0.6 mL/min.	Flow Rate 0.7 mL/min.
100	100	98	90
50	73	68	58
25	64	56	48
10	43	28	17
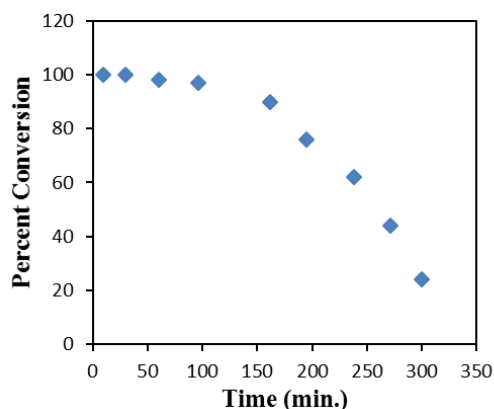
Figure 6. Catalyst half-life under optimum reaction conditions.
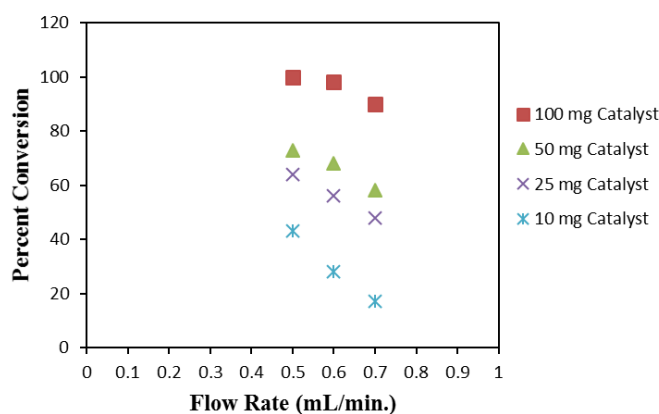
Figure 7. Catalyst loading dependency under different reaction conditions.

increasing the catalyst loading for the same flow rate lead to an increase in the conversion percentage as well.

To investigate the extent of Pd leaching from prepared catalyst, the reaction was carried out in the presence of 0.2 mol% catalyst at 100 °C for 40 min using a flow rate 0.5 mL/min. Upon the completion of the reaction period, the resulting product mixture was hot filtered and the Pd content was determined in the filtrate to be 220 ppm based on the ICP-OES analysis. Moreover, the filtrate solution was subjected to the same reaction using fresh reagents of bromobenzene and phenylboronic acid and no further catalytic activity was observed in this solution. This confirms that the catalyst is not reacting by leaching/redeposition but it is obviously in a strictly heterogeneous mode.

4. Conclusion

Applying the flow chemistry technique using X-Cube resulted in remarkable results for evaluating the catalytic activity of palladium-magnetite supported on graphene that was prepared under batch reaction conditions for being used in Suzuki cross coupling reactions of 4-bromobenzaldehyde with phenyl boronic acid. It is remarkable to notice that higher conversion rate and selectivity have been obtained in this system when compared with batch methods. This high catalytic activity is due to the role of structural defects in graphene sheets through creating new surface functionalities and hence enhances the interactions with the anchored metal nanoparticles. It is remarkable that adopting the flow chemistry approach enabled shorter time, higher conversion rate and selectivity compared to the conventional batch methods. Reaction parameters (solvent, catalyst, temperature) were rapidly optimized in the reactions. The short time of optimization allowed to a large number of optimizing reactions and facilitated generalization of the experiences. The catalyst showed high catalytic activity towards Suzuki cross - coupling reaction with 100% conversion showing that the flow chemistry provided a distinctive route of higher selectivity and conversion rate compared to the conventional batch route and also within a shorter time as it is more easy to change parameters like temperature, pressure, and flow rate and reach optimized conditions in few minutes (2-4 minutes).

Conflict of Interest

The authors declare that they have no conflict of interest.

References

[1] Radwan, M.A., Rashad, M.A., Sadek, M.A. , Elazab, H.A. (2019). Synthesis, Characterization and Selected Application of Chitosan-Coated Magnetic Iron Oxide nanoparticles. *Journal of Chemical Technology and Metallurgy*, 54(2): 303-310.

[2] De Souza, A.L.F. (2008). Microwave- and ultrasound-assisted Suzuki Miyaura cross-coupling reactions catalyzed by Pd/PVP. *Tetrahedron Letters*, 49(24): 3895-3898.

[3] Durap, F. (2009). New route to synthesis of PVP stabilized palladium(0) nanoclusters and their enhanced catalytic activity in Heck and Suzuki cross coupling reactions. *Applied Organometallic Chemistry,* 23(12): 498-503.

[4] Gniewek, A. (2005). Pd-PVP colloid as catalyst for Heck and carbonylation reactions: TEM and XPS studies. *Journal of Catalysis*, 229(2): 332-343.

[5] Ananikov, V.P. (2007). New approach for size- and shape-controlled preparation of pd nanoparticles with organic ligands. Synthesis and application in catalysis, *Journal of the American Chemical Society*, 129(23): 7252-7260.

[6] Ashfield, L. (2007). Reductive carbonylation - an efficient and practical catalytic route for the conversion of aryl halides to aldehydes. *Organic Process Research & Development*, 11(1): 39-43.

[7] Nasser, R., Radwan, M.A., Sadek, M.A., Elazab, H.A. (2018). Preparation of insulating material based on rice straw and inexpensive polymers for different roofs. *International Journal of Engineering and Technology (UAE)*, 7(4): 1989-1994.

[8] Elazab, H.A. (2019). Optimization of the Catalytic Performance of Pd/Fe$_3$O$_4$ Nanoparticles Prepared via Microwave-assisted Synthesis for Pharmaceutical and Catalysis Applications, *Biointerface Research in Applied Chemistry*, 9(1): 3794-3799.

[9] Leonhardt, S.E.S. (2006). Chitosan as a support for heterogeneous Pd catalysts in liquid phase catalysis. *Applied Catalysis A: General*, 379(1-2): 30-37.

[10] Elazab, H.A., Radwan, M.A., El-Idreesy, T.T. (2018). Facile Microwave-Assisted Synthetic Approach to Palladium Nanoparticles Supported on Copper Oxide as an Efficient Catalyst for Heck and Sonogashira Cross-Coupling Reactions, *International Journal of Nanoscience*, 17(3): 1850032-1850040.

[11] Elazab, H.A. (2014). Microwave-assisted synthesis of Pd nanoparticles supported on FeO, CoO, and Ni(OH) nanoplates and catalysis application for CO oxidation. *Journal of Nanoparticle Research*, 16(7): 1-11.

[12] Elazab, H.A. (2017). The Effect of Graphene on Catalytic Performance of Palladium Nanoparticles Decorated with FeO, CoO, and Ni (OH): Potential Efficient Catalysts Used for Suzuki Cross-Coupling. *Catalysis Letters*, 147(6): 1510-1522.

[13] Elazab, H.A. (2017). The continuous synthesis of Pd supported on Fe_3O_4 nanoparticles: A highly effective and magnetic catalyst for CO oxidation. *Green Processing and Synthesis*, 6(4): 413-424.

[14] Elazab, H.A., Sadek, M.A., El-Idreesy, T.T. (2018). Microwave-assisted synthesis of palladium nanoparticles supported on copper oxide in aqueous medium as an efficient catalyst for Suzuki cross-coupling reaction, *Adsorption Science & Technology*, 36(5-6): 1352-1365.

[15] Elazab, H.A. (2015). Highly efficient and magnetically recyclable graphene-supported Pd/Fe_3O_4 nanoparticle catalysts for Suzuki and Heck cross-coupling reactions. *Applied Catalysis A: General*, 491: 58-69.

[16] Mohsen, W., Sadek, M.A., Elazab, H.A. (2017). Green synthesis of copper oxide nanoparticles in aqueous medium as a potential efficient catalyst for catalysis applications. *International Journal of Applied Engineering Research*, 12(24): 14927-14930.

[17] Ghobashy, M., Gadallah, M., El-Idreesy, T.T., Sadek, M.A., Elazab, H.A. (2018). Kinetic Study of Hydrolysis of Ethyl Acetate using Caustic Soda. I*nternational Journal of Engineering and Technology (UAE)*, 7(4): 1995-1999.

[18] Fukui, K. (2012). Mechanism of synthesis of metallic oxide powder from aqueous metallic nitrate solution by microwave denitration method. *Chemical Engineering Journal*, 211: 1-8.

[19] Glasnov, T.N., Findenig, S., Kappe, C.O. (2009). Heterogeneous Versus Homogeneous Palladium Catalysts for Ligandless Mizoroki-Heck Reactions: A Comparison of Batch/Microwave and Continuous-Flow Processing. *Chemistry - A European Journal*, 15(4): 1001-1010.

[20] Kirschning, A., Kupracz, L., Hartwig, J. (2012). New Synthetic Opportunities in Miniaturized Flow Reactors with Inductive Heating. *Chemistry Letters*, 41(6): 562-570.

[21] Malewicz, M. (2009). Synthesis of Zinc Oxide Nanotiles by Wet Chemical Route Assisted by Microwave Heating. *Electronics Technology*, 47-50.

[22] Pourmortazavi, S.M. (2012). Synthesis, structure characterization and catalytic activity of nickel tungstate nanoparticles. *Applied Surface Science*, 263: 745-752.

[23] Elazab, H.A., Sadek, M.A., El-Idreesy, T.T. (2018). Microwave-assisted synthesis of palladium nanoparticles supported on copper oxide in aqueous medium as an efficient catalyst for Suzuki cross-coupling reaction. *Adsorption Science & Technology*, 36(5-6): 1352-1365.

[24] Yu, X.H. (2006). Research Progress of Nanostructured Materials for Heterogeneous Catalysis. *Current Nanoscience*, 7(4): 576-586.

[25] Horikoshi, S. (2006). On the Generation of Hot-Spots by Microwave Electric and Magnetic Fields and Their Impact on a Microwave-Assisted Heterogeneous Reaction in the Presence of Metallic Pd Nanoparticles on an Activated Carbon Support. *Journal of Physical Chemistry C*, 115(46): 23030-23035.

[26] Falcon, H. (2010). Large-scale synthesis of porous magnetic composites for catalytic applications, in Scientific Bases for the Preparation of Heterogeneous Catalysts: *Proceedings of the 10th International Symposium, E.M. Gaigneaux*, 347-350.

[27] Chen, S.T. (2012). Synthesis of Pd/Fe_3O_4 Hybrid Nanocatalysts with Controllable Interface and Enhanced Catalytic Activities for CO Oxidation. *Journal of Physical Chemistry C*, 116(23): 12969-12976.

[28] Moussa, S., Abdelsayed, V., El-Shall M.S. (2011). Laser synthesis of Pt, Pd, CoO, and Pd-CoO nanoparticle catalysts supported on graphene. *Chemical Physics Letters*, 510(4-6): 179-184.

[29] Qiu, G.H. (2011). Microwave-Assisted Hydrothermal Synthesis of Nanosized alpha-Fe2O3 for Catalysts and Adsorbents. *Journal of Physical Chemistry C*, 115(40): 19626-19631.

[30] Wang, H.L. (2010). $Ni(OH)_2$ Nanoplates Grown on Graphene as Advanced Electrochemical Pseudocapacitor Materials. *Journal of the American Chemical Society*, 132(21): 7472-7477.

[31] Wang, H.L. (2010). Nanocrystal Growth on Graphene with Various Degrees of Oxidation. *Journal of the American Chemical Society*, 132(10): 270-285.

[32] Kalbasi, R.J., Negahdari, M. (2006). Synthesis and characterization of mesoporous poly(N-vinyl-2-pyrrolidone) containing palladium nanoparticles as a novel heterogeneous organocatalyst for Heck reaction. *Journal of Molecular Structure*, 1063: 259-268.

[33] Martins, D.d.L. (2009). Heck reactions catalyzed by Pd(0)-PVP nanoparticles under conventional and microwave heating. *Applied Catalysis A: General*, 408(1): 47-53.

[34] Sheng, L. (2006). PVP-coated graphene oxide for selective determination of ochratoxin A via quenching fluorescence of free aptamer. *Biosensors and Bioelectronics*, 26(8): 3494-3499.

[35] Zhang, J., Bai, X. (2010). Microwave-assisted synthesis of Pd nanoparticles and their catalysis application for Suzuki cross-coupling reactions. I*norganic and Nano-Metal Chemistry*, 47(5): 672-676.

[36] Elazab, H.A. (2018). The catalytic activity of copper oxide nanoparticles towards carbon monoxide oxidation catalysis: microwave assisted synthesis approach, *Biointerface Research in Applied Chemistry*, 8(3): 3278-3281.

[37] Zhang, Y. (2011). One-step synthesis of Polyvinylpyrrolidone-reduced graphene oxide-Pd nanoparticles for electrochemical sensing. *Journal of Materials Science*, 51(13): 6497-6508.

[38] Nicolaou, K.C., Bulger, P.G., Sarlah, D. (2005). Palladium-catalyzed cross-coupling reactions in total synthesis. *Angewandte Chemie-International Edition*, 44(29): 4442-4489.

[39] Ashraf, B., Elazab, H.A. (2018). Preparation and characterization of decorative and heat insulating floor tiles for buildings roofs. *International Journal of Engineering and Technology (UAE)*, 7(3): 1295-1298.

[40] Elazab, H.A. (2018). Laser vaporization and controlled condensation (LVCC) of graphene supported Pd/Fe_3O_4 nanoparticles as an efficient magnetic catalysts for Suzuki Cross Coupling. *Biointerface Research in Applied Chemistry*, 8(3): 3314-3318.

[41] Mankarious, R.A., Elazab, H.A. (2017). Bulletproof vests/shields prepared from composite material based on strong polyamide fibers and epoxy resin. *Journal of Engineering and Applied Sciences*, 12(10): 2697-2701.

[42] Mostafa, A.R., Omar, H.A.-S., Elazab, H.A. (2017). Preparation of Hydrogel Based on Acryl Amide and Investigation of Different Factors Affecting Rate and Amount of Absorbed Water. *Agricultural Sciences*, 8(2): 11-18.

[43] Radwan, M.A., Elazab, H.A. (2017). Mechanical characteristics for different composite materials based on commercial epoxy resins and different fillers, *Journal of Engineering and Applied Sciences*, 12(5): 1179-1185.

[44] Samir, N.S., Elazab Hany. (2018). Preparation and characterization of bulletproof vests based on polyamide fibers. *International Journal of Engineering and Technology (UAE)*, 7(3): 1290-1294.

[45] Elazab, H.A. (2019). Investigation of Microwave-assisted Synthesis of Palladium Nanoparticles Supported on Fe_3O_4 as an Efficient Recyclable Magnetic Catalysts for Suzuki Cross-Coupling, *The Canadian Journal of Chemical Engineering*, 97(5): 225-234.

[46] Zakaria, F., Radwan, M.A., Sadek, M.A., Elazab, H.A. (2018). Insulating material based on shredded used tires and inexpensive polymers for different roofs. *International Journal of Engineering and Technology (UAE)*, 7(4):1983-1988.